Atomic sublattice decomposition of piezoelectric response in tetragonal $PbTiO_3$, $BaTiO_3$, and $KNbO_3$

Jing Shi,[1,2] Ilya Grinberg,[2] Xiaoli Wang,[1,*] and Andrew M. Rappe[2,†]

[1]*MOE Key Laboratory for Nonequilibrium Synthesis and Modulation of Condensed Matter, School of Science, Xi'an Jiaotong University, Xi'an 710049, People's Republic of China*

[2]*The Makineni Theoretical Laboratories, Department of Chemistry, University of Pennsylvania, Philadelphia, Pennsylvania 19104-6323, USA*

(Received 26 September 2013; published 21 March 2014)

The piezoelectric properties of tetragonal perovskites $PbTiO_3$, $BaTiO_3$, and $KNbO_3$ under uniaxial strain along the [001] direction are calculated from first principles. In order to study the piezoelectric response of individual atomic sublattices, the total polarization P and piezoelectric constant d_{33} are decomposed into the contributions of A-site and B-site atoms. These three materials show different behaviors at the atomic scale. In $PbTiO_3$, the Pb and Ti contribute almost equally to the polarization and d_{33}. In $KNbO_3$, most of the polarization and d_{33} are contributed by the ferroelectrically active Nb. But in $BaTiO_3$, as the c axis increases, the contribution of Ba to d_{33} rises rapidly, reaching 50% of the total d_{33} at $c = 4.30$ Å. This means that the covalent bonding between Ba and O is significant and has an important impact on the piezoelectric response of $BaTiO_3$.

DOI: 10.1103/PhysRevB.89.094105 PACS number(s): 77.84.Lf, 71.15.−m, 71.20.−b

I. INTRODUCTION

Lead-based piezoelectric materials are widely investigated due to their important device applications, such as ferroelectric memories, microelectronic devices, and ultrasound transducers. The Pb off-centering displacement has a crucial effect on the high performance of the lead-based materials [1–4]. Currently, much effort is being invested in the search for lead-free piezoelectric materials with large piezoelectric constant d_{33} and higher Curie temperature [5–8]. In recent years, both $BaTiO_3$- and (K, Na)NbO_3-based materials have been intensively studied as promising candidates to replace lead-based materials. This has led to the discovery of solid solutions with large d_{33}, for example, $BaZrO_3$-$BaTiO_3$ [9], $CaTiO_3$-$BaTiO_3$ [10], Ba(Zr,Ti)O_3-(Ba,Ca)TiO_3 [11], $K_{0.5}Na_{0.5}NbO_3$-$LiTaO_3$ [12], and $K_{0.5}Na_{0.5}NbO_3$-$LiNbO_3$ [13]. Since cation compositional change is the primary tool for design of these materials, a firm understanding of how individual cations contribute to the overall piezoelectric response of the materials would help the rational design of high-performance piezoelectrics.

In this study, we use first principles calculations to resolve the contributions of the A-site and B-site sublattices to the piezoelectric properties of the classic tetragonal $PbTiO_3$, $BaTiO_3$, and $KNbO_3$ materials in the ground state and under tetragonal expansion. We found that the A-site atoms of Pb, Ba, and K show different piezoelectric response behaviors, due to the different bonding nature with O. To our knowledge, our work is the first calculation of the piezoelectric contributions of individual atomic sublattices in piezoelectric materials.

II. METHODOLOGY

The electronic structure calculations presented here are conducted using density functional theory [14] as implemented in the Quantum Espresso code [15]. All calculations were performed with a plane-wave basis set with an energy cutoff of 60 Ry. The local density approximation [16] and an $8 \times 8 \times 8$ Monkhorst-Pack k-point mesh were used in the calculations. All atoms are represented by norm-conserving optimized nonlocal pseudopotentials generated by the OPIUM code [17]. The calculations were sufficiently converged to allow the atomic structures to be optimized until the residual forces on the atoms are less than 5 meV/Å.

Various amounts of strain along the [001] direction were applied to $PbTiO_3$, $BaTiO_3$, and $KNbO_3$. The lattice vectors perpendicular to the [001] direction and all the internal atomic positions are optimized. The minimization is continued until the other two components of the stress tensor (i.e., σ_{11} and σ_{22}) are all smaller than 0.01 GPa. After optimization, the corresponding polarization was calculated by the Berry phase method [18].

A finite difference method was used to calculate the d_{33} of each structure, according to the piezoelectric equation $d_{33} = dP/d\sigma_3$, where P is the polarization and σ is the stress. ±0.5% strains were used as the perturbations, and the perturbed structures were optimized as before.

In order to obtain the individual atomic sublattice contributions to the d_{33}, we first decomposed the total polarization into the contributions from the A-site and B-site atoms [19]. The A-site and B-site polarization contributions are calculated by $P(A) = \bar{Z}^*_{33}(A) \times D(A)$ and $P(B) = \bar{Z}^*_{33}(B) \times D(B)$, where $\bar{Z}^*_{33}(A)$ and $\bar{Z}^*_{33}(B)$ are the average Born effective charges between paraelectric and ferroelectric structures as calculated by DFT, and D is the off-center displacement from the center of the corresponding O cage. Then the contributions of A-site and B-site atoms to the total d_{33} can be calculated as $d_{33}(A) = dP(A)/d\sigma_3$ and $d_{33}(B) = dP(B)/d\sigma_3$.

In the perovskite structure, A-site and B-site atoms are located in the O_{12} and O_6 cages, respectively. Their piezoelectric response abilities are related to the bonding with the surrounding O atoms. In our method, the polarization and piezoelectric constant decompositions are calculated from the Born effective charges and the displacements from the corresponding O cages, so the O contribution is already included in the $d_{33}(A)$ and $d_{33}(B)$.

*xlwang1@mail.xjtu.edu.cn
†rappe@sas.upenn.edu

TABLE I. Lattice constants (Å), effective charges (e), polarizations (C/m^2), polarization decomposition (C/m^2), piezoelectric constants (pC/N), and d_{33} decomposition (pC/N) of the ground state $PbTiO_3$, $BaTiO_3$, and $KNbO_3$.

	$PbTiO_3$	$BaTiO_3$	$KNbO_3$
a	3.859	3.942	3.955
c	4.056	3.990	4.036
$Z^*_{33}(A)$	3.55	2.80	1.13
$Z^*_{33}(B)$	5.55	6.33	7.36
P	0.838	0.270	0.385
$P(A)$	0.402	0.047	0.033
$P(B)$	0.385	0.204	0.353
d_{13}	−15	−9	−7
d_{33}	80	43	29.8
$d_{33}(A)$	38	9.7	3.4
$d_{33}(B)$	42	29.3	23.8
$d_{33}(A)/d_{33}(B)$	0.905	0.331	0.143

III. RESULTS AND DISCUSSIONS

The calculated lattice constants, effective charges, polarization and piezoelectric constants of the ground state $PbTiO_3$, $BaTiO_3$, and $KNbO_3$ structures are listed in Table I. Those results are in good agreement with previous DFPT calculations [20–23]. The decompositions of polarization and d_{33} to atomic sublattice are also included in Table I, and the sum of the decomposed atomic components is in good agreement with the value obtained by the standard d_{33} definition.

The polarization decomposition data show strong differences between the A-site atoms. For $PbTiO_3$, the polarization contributions from Pb and Ti are nearly the same, with the larger displacement of Pb balanced by its lower Born effective charge. For both Pb and Ti, the Born effective charges are anomalously large due to the presence of strong hybridization of Pb 6s and Ti 3d orbitals with O 2p orbitals [1]. In $BaTiO_3$ and $KNbO_3$, most of the polarization comes from the B-site Ti and Nb, because of the strong hybridization of the Ti 3d and Nb 4d orbitals with the O 2p orbitals [24]. A-site Ba and K contribute little to the total polarization. The polarization contribution of K is the smallest ($\leq$9% of the total polarization), due to the essentially ionic interaction between K and O. The Born effective charge of K is 1.13, which is nearly the same as its oxidation state.

The d_{33} decomposition results are related to the polarization decomposition. In $PbTiO_3$, the total d_{33} is 80 pC/N, and the contributions from Pb and Ti are nearly identical—38 and 42 pC/N, respectively. The total d_{33} of $BaTiO_3$ and $KNbO_3$ are 42 and 29.8 pC/N. In $BaTiO_3$, Ba contributes 9.7 pC/N and Ti contributes 29.3 pC/N. In $KNbO_3$, K contributes only 3.4 pC/N and Nb contributes 23.8 pC/N. Both in $BaTiO_3$ and $KNbO_3$, the contributions from B-site Ti and Nb are much larger than the A-site Ba and K. The d_{33}(Ba) is nearly three times larger than d_{33}(K), and d_{33}(Ti) is nearly the same as d_{33}(Nb). The piezoelectric response of K is highly suppressed by the ionic interaction between K and O.

We now analyze the effects of the c-axis changes on the polarization, piezoelectric constant d_{33}, and their decompositions. Figure 1 shows the results for the total polarizations

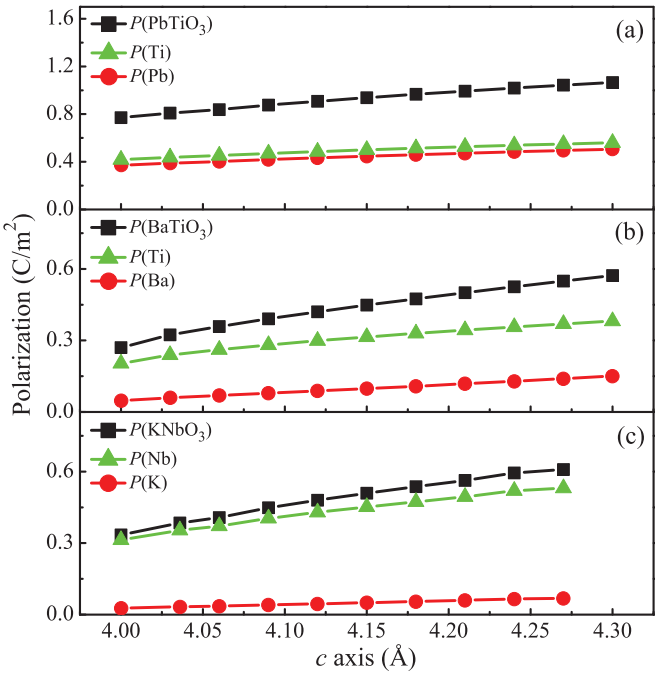

FIG. 1. (Color online) Polarization and atomic sublattice decomposition of polarization (a) $PbTiO_3$, (b) $BaTiO_3$, and (c) $KNbO_3$ versus c-axis length.

of $PbTiO_3$, $BaTiO_3$, and $KNbO_3$ and their decompositions versus c-axis length. In $PbTiO_3$, Pb and Ti contributions are very similar for all values of c. In $KNbO_3$, with c increasing from 4.00 Å to 4.27 Å, the polarization contribution from K increases very slowly from 8% to 11%; for all c values the vast majority of polarization is contributed by Nb. However, in $BaTiO_3$ the fraction of the total polarization contributed

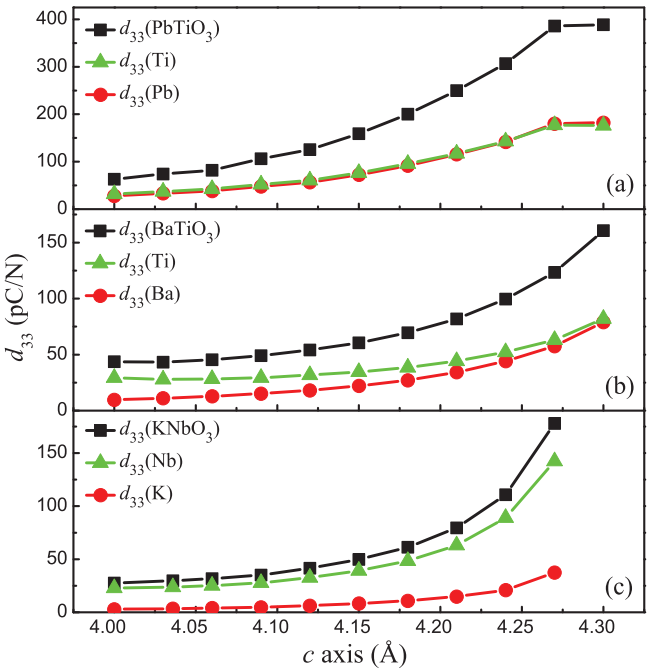

FIG. 2. (Color online) d_{33} and atomic sublattice decomposition of d_{33} of (a) $PbTiO_3$, (b) $BaTiO_3$, and (c) $KNbO_3$ versus c-axis length.

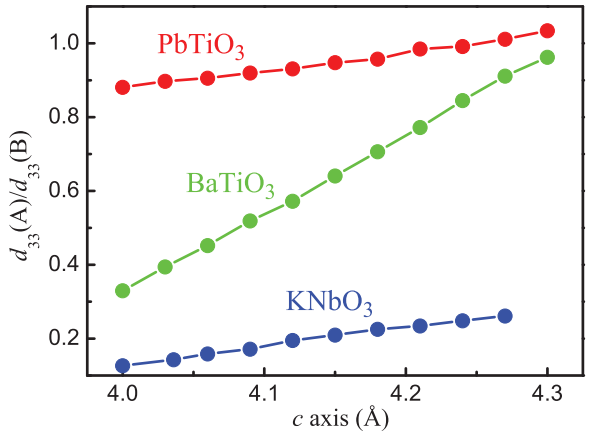

FIG. 3. (Color online) The d_{33} contribution ratio of A-site and B-site atoms versus c-axis length in $PbTiO_3$, $BaTiO_3$, and $KNbO_3$.

by the A-site Ba rises significantly at large strains. While at $c = 4.00$ Å Ba contributes 12% of the total polarization, at $c = 4.30$ Å the fraction of total polarization contributed by Ba doubles to 25%. The strong enhancement of the Ba contribution at larger strains is even more pronounced in the d_{33} data (Fig. 2). As c increases, Ba d_{33}(Ba) rises rapidly and reaches 50% of the total d_{33} at $c = 4.30$ Å. By contrast, for $PbTiO_3$ and $KNbO_3$ the fractions of the total d_{33} from the A- and B-sites stay nearly the same, even as the overall d_{33} rises with increased lattice constant c. The different piezoelectric response behaviors of Ba and K indicate that the bonding behaviors of Ba-O and K-O are different.

To illustrate the differences between the three materials, we plot the ratios of the calculated A- and B-site d_{33} contributions $d_{33}(A)/d_{33}(B)$ in Fig. 3. For all three materials, $d_{33}(A)/d_{33}(B)$ increases almost linearly with increasing c. For $BaTiO_3$, it shows different behavior from $PbTiO_3$ and $KNbO_3$. As c increases, the contribution of Ba increases much faster than the contribution of Ti, and the d_{33}(Ba)/d_{33}(Ti) increases rapidly from 0.33 to 0.96.

We assign this activation of d_{33}(Ba) to the covalent bonding between Ba and the corresponding O_{12} cage. The Ba-O bond is typically thought of as ionic, similar to the K-O bond in $KNbO_3$. In our calculations the Born effective charge of Ba is 2.80 at $c = 4.00$ Å and 2.92 at $c = 4.30$ Å, clearly larger than the formal charge of 2.0. This suggests that the Ba-O interaction is not purely ionic. Partial covalency of the Ba-O bond has been studied both in experiments [25] and by first principles calculations [26]. In order to investigate the relationship between the anomalous increase of d_{33}(Ba) and the bonding behavior of the Ba and the surrounding O atoms, we calculated the charge density of the (100) plane of $BaTiO_3$ at $c = 4.00$ Å and $c = 4.30$ Å, as shown in Fig. 4. At $c = 4.00$ Å, Ba hybridizes with all the nearest 12 O atoms. At $c = 4.30$ Å, the Ba-O bonding environment changes; the Ba-O bonding is enhanced along the Ba displacement direction and disappears in the opposite direction. This bonding

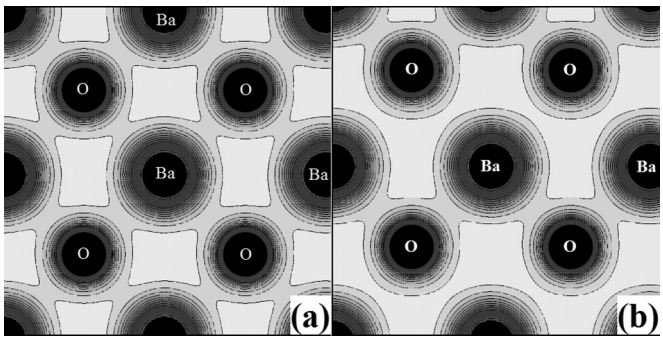

FIG. 4. Charge density of (100) plane in $BaTiO_3$ at (a) $c = 4.0$ Å and (b) $c = 4.3$ Å.

configuration makes Ba more responsive to the external strain (or stress) and gives rise to a large Ba contribution to the total d_{33} in $BaTiO_3$. At $c = 4.30$ Å, the d_{33}(Ba) from Ba becomes comparable with d_{33}(Ti) that is from the ferroelectrically active Ti. This hidden enhanced piezoelectric response of Ba in $BaTiO_3$ may be realized experimentally by growing $BaTiO_3$ on a substrate with smaller lattice parameters, in order to induce a large tetragonality.

IV. CONCLUSION

We have calculated the polarization and d_{33} of the tetragonal structures of $PbTiO_3$, $BaTiO_3$, and $KNbO_3$ as a function of c-axis length. We also decomposed the polarization and d_{33} to the contributions of the A-site and B-site atoms. In $PbTiO_3$, Pb and Ti make comparable contributions to the total d_{33}. In $KNbO_3$, the total d_{33} mostly comes from Nb, but in $BaTiO_3$, the contribution of Ba increases rapidly with c-axis increase. This is caused by covalent bonding between Ba $5p$ and O $2p$ orbitals. Our work shows that decomposition of the piezoelectric response into the contributions of the individual cation-oxygen cages can shed light on the microscopic origins of material piezoelectricity. We hope that this approach will be useful in the studies of complex solid-solution piezoelectrics and in the design of new high-performance piezoelectric materials.

ACKNOWLEDGMENTS

J.S. was supported by the scholarship from China Scholarship Council (CSC) under the CSC Grant No. 2010628086. I.G. was supported by the Office of Naval Research, under Grant No. N00014-12-1-1033. A.M.R. was supported by the Department of Energy Office of Basic Energy Sciences, under Grant No. DE-FG02-07ER46431. Computational support was provided by the High-Performance Computing Modernization Office (HPCMO) of the US Department of Defense and by the National Energy Research Science Computing Center (NERSC) of the US Department of Energy.

[1] R. E. Cohen, Nature **358**, 136 (1992).
[2] L. Bellaiche and D. Vanderbilt, Phys. Rev. Lett. **83**, 1347 (1999).
[3] Z. Wu and R. E. Cohen, Phys. Rev. Lett. **95**, 037601 (2005).

[4] P. Baettig, C. F. Schelle, R. LeSar, U. V. Waghmare, and A. Spaldin, Chem. Mater. **17**, 1376 (2005).
[5] Y. Saito, H. Takao, T. Tani, T. Nonoyama, K. Takatori, T. Homma, T. Nagaya, and M. Nakamura, Nature **432**, 84 (2004).
[6] A. Herabut and A. Safari, J. Am. Ceram. Soc. **80**, 2954 (1997).
[7] S. Zhang and F. Yu, J. Am. Ceram. Soc. **94**, 3153 (2011).
[8] M. Matsubara, K. Kikuta, and S. Hirano, J. Appl. Phys. **97**, 114105 (2005).
[9] Z. Yu, R. Guo, and A. S. Bhalla, Appl. Phys. Lett. **77**, 1535 (2000).
[10] D. Fu, M. Itoh, and S. Koshihara, Appl. Phys. Lett. **93**, 012904 (2008).
[11] W. Liu and X. Ren, Phys. Rev. Lett. **103**, 257602 (2009).
[12] E. Hollenstein, M. Davis, D. Damjanovic, and N. Setter, Appl. Phys. Lett. **87**, 182905 (2005).
[13] Y. Guo, K. Kakimoto, and H. Ohsato, Appl. Phys. Lett. **85**, 4121 (2005).
[14] W. Kohn and L. J. Sham, Phys. Rev. **140**, A1133 (1965).
[15] P. Giannozzi, S. Baroni, N. Bonini, M. Calandra, R. Car, C. Cavazzoni, D. Ceresoli, G. L. Chiarotti, M. Cococcioni, I. Dabo *et al*., J. Phys.: Condens. Matter **21**, 395502 (2009).
[16] J. P. Perdew and A. Zunger, Phys. Rev. B **23**, 5048 (1981).
[17] http://opium.sourceforge.net.
[18] D. Vanderbilt and R. D. King-Smith, Phys. Rev. B **48**, 4442 (1993).
[19] I. Grinberg and A. M. Rappe, Phys. Rev. Lett. **98**, 037603 (2007).
[20] C. J. Yu and H. Emmerich, J. Phys.: Condens. Matter **19**, 306203 (2007).
[21] Y. Duan, H. Shi, and L. Qin, J. Phys.: Condens. Matter **20**, 175210 (2008).
[22] Y. Duan, G. Tang, C. Chen, T. Lu, and Z. Wu, Phys. Rev. B **85**, 054108 (2012).
[23] L. F. Wan, T. Nishimatsu, and S. P. Beckman, J. Appl. Phys. **111**, 104107 (2012).
[24] M. Posternak, R. Resta, and A. Baldereschi, Phys. Rev. B **50**, 8911 (1994).
[25] P. Ghosez, X. Gonze, P. Lambin, and J. P. Michenaud, Phys. Rev. B **51**, 6765 (1995).
[26] L. T. Hudson, R. L. Kurtz, S. W. Robey, D. Temple, and R. L. Stockbauer, Phys. Rev. B **47**, 1174 (1993).